SCIENTIFIC REPORTS

OPEN

SUBJECT AREAS:
GENE REGULATION
TRANSLATION
PATHOLOGY
ANIMAL BEHAVIOUR

Received
31 October 2011

Accepted
23 February 2012

Published
19 March 2012

Correspondence and requests for materials should be addressed to O.O. (ogawao@kuhp.kyoto-u.ac.jp)

BALB/c-*Fcgr2b*$^{-/-}$*Pdcd1*$^{-/-}$ mouse expressing anti-urothelial antibody is a novel model of autoimmune cystitis

Yoshio Sugino[1], Nobuyuki Nishikawa[1], Koji Yoshimura[1], Sadako Kuno[2], Yukio Hayashi[3], Naoki Yoshimura[3], Taku Okazaki[4], Akihiro Kanematsu[1] & Osamu Ogawa[1]

[1]Department of Urology, Kyoto University, Kyoto, Japan, [2]Department of Neurology, National Center of Neurology and Psychiatry, Musashi Hospital, Tokyo, Japan, [3]Department of Urology, University of Pittsburgh School of Medicine, Pittsburgh, USA, [4]Division of Immune Regulation, Institute for Genome Research, The University of Tokushima, Tokushima, Japan.

We report the impact of anti-urothelial autoantibody (AUAb) on urinary bladder phenotype in BALB/c mice deficient of the FcγRIIb and PD-1. AUAb was present in serum samples from approximately half of the double-knockout (DKO) mice, as detected by immunofluorescence and immunoblots for urothelial proteins including uroplakin IIIa. The AUAb-positive DKO mice showed degeneration of urothelial plaque and umbrella cells, along with infiltration of inflammatory cells in the suburothelial layer. TNFα and IL-1β were upregulated in the bladder and the urine of AUAb-positive DKO mice. Voiding behavior of mice was analyzed by the Voided Stain on Paper method. 10-week-old and older AUAb-positive DKO mice voided significantly less urine per void than did wild type (WT) mice. Furthermore, administration of the AUAb-containing serum to WT mice significantly reduced their urine volume per void. In summary, this report presents a novel comprehensive mouse model of autoimmune cystitis.

An autoimmune mechanism has been postulated as a candidate cause for non-bacterial inflammatory diseases of the bladder such as interstitial cystitis, eosinophilic cystitis and lupus cystitis in human[1–3]. However, direct mechanistic association between autoimmune processes and functional changes in the bladder has not been established clinically. In experimental model, administration of exogenous molecule has been shown to elicit inflammatory change in the bladder[4]. Further, recent studies described the mechanism of autoimmune responses in the bladder by analyzing transgenic mice that constitutively express a self-antigen in the bladder epithelium, but did not elucidate whether the autoantibody could be pathogenic for bladder function in behavioral level or not[5,6]. In short, role of autoimmune processes in bladder pathophysiology is yet incompletely elucidated.

During the storage of urine in the bladder, umbrella cells, which are located on the surface of the bladder epithelium (urothelium), play an important role in the bladder barrier function[7]. Uroplakin (UPK) Ia, Ib, II, and IIIa are components of urothelial cell plaques, whose function is to reduce the transcellular passage of water through the urothelium[8]. Mice defective of UPKs show elevated water permeability in the urothelium[9], vesicoureteral reflux, hydronephrosis[10] and decreased bladder capacity[11], demonstrating the importance of these barrier molecules in normal bladder function. Recent study showed that immunization with recombinant mouse UPK II might cause bladder specific inflammation and urinary frequency, though this study failed to describe any histological changes in urothelium, which includes UPK II proteins[12].

The BALB/c mouse deficient in low affinity type IIb Fc receptor for IgG (FcγRIIB or *Fcgr2b*) and programmed cell death 1 (PD-1 or *Pdcd*-1) (BALB/c-*Fcgr*2b$^{-/-}$*Pdcd*1$^{-/-}$ mouse / the DKO mouse) exhibits autoimmune phenotypes including autoimmune dilated cardiomyopathy[13] and gastritis[14]. Interestingly, serum samples derived from the DKO mice also react to the urothelium and to UPKIIIa, and hydronephrosis is reported as a phenotypic consequence of anti-urothelial autoantibody (AUAb) due to periureteral inflammation[14]. As an extension of this study, we hypothesized that ablation of urothelium by the autoantibody should also impair bladder function. Therefore we analyzed the bladder of DKO mice to examine impact of the anti-urothelial antibody (AUAb), using biological and physiological techniques including a method reported as "Voided Stain on Paper (VSOP) method"[15], and demonstrate here a novel comprehensive mouse model of autoimmune cystitis.

Results

Expression of AUAb in DKO mice. The presence of AUAb in serum samples was detected using mouse serum as primary antibodies for immunofluorescence (IF) of WT mouse bladder (Supplementary Fig. 1A) and immunoblotting for UPKIIIa, a component of urothelial plaque (Supplementary Fig. 1B)[14]. AUAb in serum of the DKO mice could be detected as early as 7 weeks of age by the IF. At 10-week-old, approximately half of DKO mice (7/13; 53.8%) expressed AUAb (Supplementary Fig. 1A right), but no WT mice did (0/10; 0%, Supplementary Fig. 1A left). In addition, the DKO mouse serum with positive immunoreactivity for the urothelium by IF, also recognized uroplakin 3A (UPKIIIa) by immunoblotting, indicating that UPKIIIa is one of the target proteins of AUAb (Supplementary Fig. 1B).

These AUAb-positive DKO mice remained positive until 16-week-old, while no new AUAb-positive mice appeared after 10-week. The positive rate of AUAb in the serum samples from DKO mice varied by the colony as shown in the former and current studies (35.3% and 53.8%, respectively)[14].

DKO mice expressing AUAb have degenerated urothelium. We then evaluated the impact of AUAb on bladder morphology, by comparing wild-type mice, DKO mice with AUAb (AUAb-positive DKO mice), and those without AUAb (AUAb-negative DKO mice). There was marked disarrangement of urothelial plaque on the surface of the bladder of AUAb-positive DKO mice, but not in WT or AUAb-negative DKO mice (Fig. 1A–I). Hematoxylin and eosin (H&E) staining, and more prominently scanning electron microscopy (SEM), showed a disarranged cellular structure of the bladder epithelium in AUAb-positive DKO mice at 16-week-old compared to WT mice or AUAb-negative DKO mice (Fig. 1A, B and D, E). The surface of bladder epithelium from AUAb-positive DKO mice exhibited poorer plaque formation, exposing bare surface of smaller epithelial cells beneath it (Fig. 1E). This morphological difference correlated with weaker staining of UPKIIIa in the bladders of AUAb-positive DKO mice compared to bladders from WT or AUAb-negative DKO mice (Fig. 1G, H, and I).

These morphological features showed a close similarity to that of UPKIII KO mice reported by Hu et al.[10], suggesting that AUAb may cause immunological ablation of UPKIII and apical cell layer of the urothelium.

Infiltration of inflammatory cells at the suburothelial layer of AUAb-positive DKO mice. The other remarkable morphological feature in the AUAb-positive DKO mice was massive infiltration of inflammatory cells in the suburothelial layer, which was never observed in WT or AUAb-negative DKO mice (Fig. 2A–C). There was marked infiltration of c-kit-positive inflammartory cells into the suburothelial layer of AUAb-positive DKO mice (Fig. 2D-F). The c-kit-positive cell count was significantly elevated in AUAb-positive DKO mice compared with AUAb-negative DKO or WT mice (Fig. 2G). Although c-kit has been known as a marker for mast cells[16], these c-kit-positive cells did not have typical morphological feature of mast cells. There were also inflammatory cells positively stained for CD4 (T cell marker), CD11c (dendritic cell marker) and B220 (activated B cell marker) (Fig. 2I, K, M), while immunoreactivity for F4/80, which is the marker of macrophage was not elevated (Fig. 2O).

Expression of inflammatory cytokines in the suburothelial layer. In addition to morphological analyses, we analyzed the inflammatory process by identifying inflammatory factors using PCR analyses. TaqMan low-density array (TLDA) showed that mRNA expression levels of six molecules (*Il2ra, Tnf, Icos, Il1b, Socs1, Vcam1*) were significantly upregulated in the bladder of AUAb-positive DKO mice, as compared to WT mice (Supplementary Fig. 2A: $p<0.01$). Meanwhile, ELISA assay for urinary cytokines revealed that the protein level of seven molecules (GM-CSF, TNFα, IL-1α, G-CSF, IL-1β, RANTES, MIP-1β) was significantly upregulated in the urine of AUAb-positive DKO mice, as compared to WT mice (Supplementary Fig. 2B: $p<0.05$). Consequently, two molecules, TNFα and IL-1β were elevated in both bladder mRNA and urine protein levels (Fig. 3A). Of these, TNFα is known as a major mediator

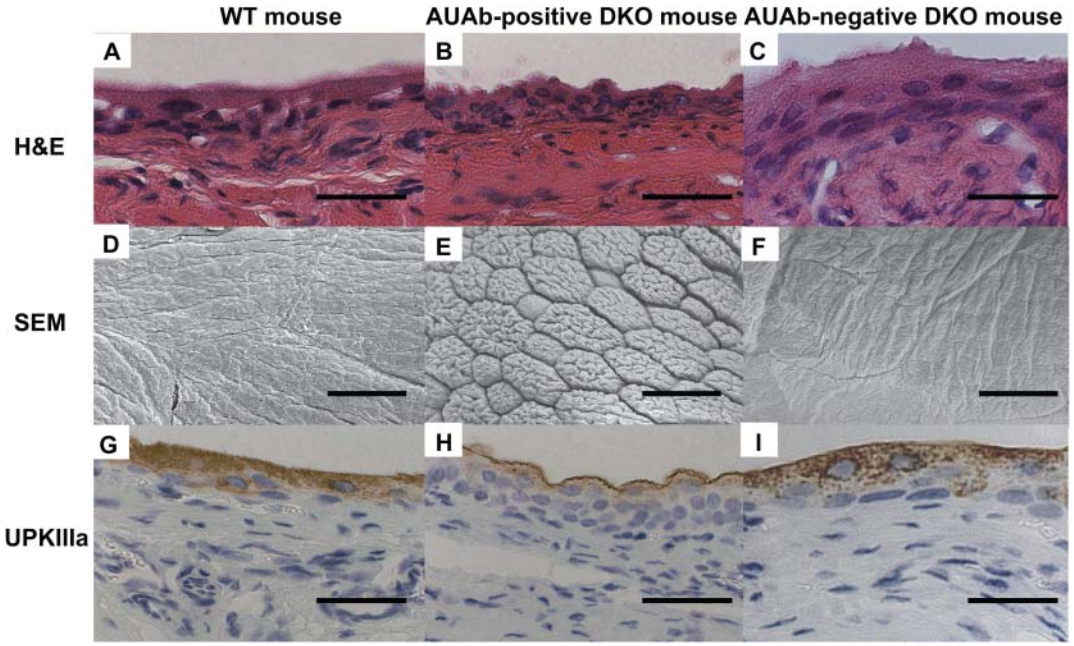

Figure 1 | DKO mice expressing AUAb have degenerated urothelium. Histological analyses of bladder tissue of WT (A, D, G), AUAb-positive DKO (B, E, H), and AUAb-negative DKO (C, F, I) mice are displayed. (A–C) Hematoxylin and eosin (H&E) stain showed smaller epithelial cells including umbrella cells in the bladder of AUAb-positive DKO mice (B) than WT (A) and AUAb-negative DKO mice (C). (D–F) Scanning electron microscopy (SEM) revealed epithelial plaque in the bladder of WT (D) and AUAb-negative DKO mice (F); however, the size of plaques was decreased in AUAb-positive DKO mice (E). (G–I) The intensity of staining for UPKIIIa was reduced in the urothelial layer of AUAb-positive DKO mice (H) compared to WT (G) and AUAb-negative DKO mice (I). Bars indicate 30 μm in A–C, G–I, 10 μm in D–F.

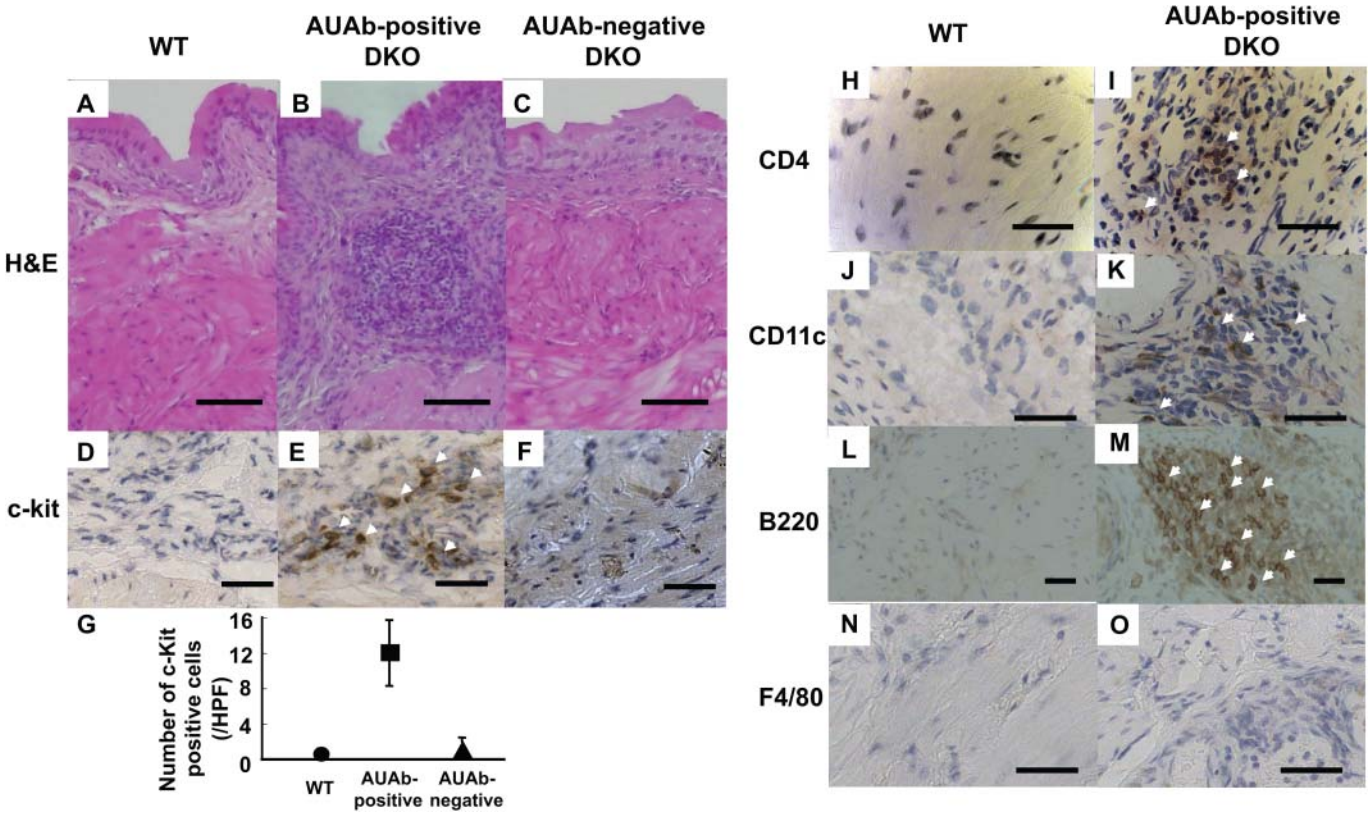

Figure 2 | C-Kit expressing cells are significantly elevated in the suburothelial layer of AUAb-positive DKO mice. (A–F) H&E staining (A–C) and immunohistochemistry for c-Kit (D–F) are shown. There were many inflammatory cells beneath the urothelium of AUAb-positive DKO mice and c-Kit-positive cells were observed in the lesion (B, E), though there were no infiltration of inflammatory cells nor c-Kit-positive cells in the specimen of WT (A, D) and AUAb-negative DKO (C, F) mice. (G) There was a significant increase in the number of c-Kit-positive cells in the bladder of AUAb-positive DKO mice (■: n=5) compared to WT (●: n=5) and AUAb-negative DKO mice (▲: n=5) under microscopic observation (**$p<0.01$).
(H–O) Immunohistochemistry for the other important inflammatory cells is shown for bladder of WT (H, J, L, N) and AUAb-positive DKO mice (I, K, M, O). CD4 (T-cell marker: H, I), CD11c (dendritic cell marker: J, K) and B220 (activated B-cell marker: L, M) were prominent in the bladder of AUAb-positive DKO mice (I, K, M) compared to the WT bladder that had no infiltration of inflammatory cells (H, J, L) (positive cells are indicated by white arrows), while there were no remarkable staining of F4/80 (macrophage marker: N, O) in AUAb-positive DKO bladder (O) and there were no infiltration of inflammatory cells in WT bladder (N). Bars indicate 100 μm in A–C, 30 μm in D–F, H–O.

of inflammation and an important therapeutic target of autoimmune diseases such as rheumatoid arthritis or inflammatory bowel disease[17,18], and is also reported to play a crucial role in the pathology of inflammatory diseases of the bladder in animal models of neurogenic cystitis[19,20]. In the AUAb-positive DKO mice, the *tnf* mRNA expression level was upregulated in the stomach and the bladder, suggesting that the inflammatory process is not systemic, but involved limited number of organs, against which specific antibody is expressed, the stomach[14] and the bladder (Fig. 3B).

Another separate ELISA study replicated the finding that urine of AUAb-positive DKO mice contained a significantly higher level of TNFα compared to WT mice (Fig. 3C: $p<0.05$). This elevated urine TNFα (Fig. 3C) may not derive from the kidney, but should account for overexpression of this molecule in the diseased bladder, since it was neither elevated in the kidney nor in the serum, (Fig. 3B).

In summary, the elevation of the inflammatory mediators including TNFα indicated the significance of inflammation process in the bladder of AUAb-positive DKO mice, which made us to focus on the phenotype in context of the bladder function.

Presence of AUAb in the serum is associated with impaired bladder storage function. To evaluate the behavioral consequence of the inflammation in AUAb-positive mice, we analyzed urination of the mice by a method reported as 'VSOP method' by us[15]. From 10 to 16- week-old, the AUAb-positive DKO mice (n=7) voided significantly less urine per void than did WT mice (n=10, $p<0.01$), while there were no significant differences between AUAb-negative DKO (n=6) and the WT mice (Fig. 4A upper). Because AUAb-positive DKO mice had lower body weight than WT mice, we also examined the data with correction by body weight, and confirmed that the urine volume per void of AUAb-positive DKO mice was still significantly smaller than that of WT mice (Fig. 4A middle). The significant difference was also noted when the urine volume per void was adjusted as the ratio against the urine volume per void in 4-week-old (urine volume per void index, Fig 4A lower). Urine volume per void of AUAb-negative DKO mice showed slight and transient decrease compared to WT, but did not reach statistical significance except on the weight-adjusted data at 10-week-old (Fig. 4A middle), suggesting that presence of AUAb had greater impact on the bladder function than the genetic modification itself.

Based on these findings, we examined whether AUAb-containing serum is a pathogenic factor by itself in animals without genetic alteration. Intraperitoneal administration of the AUAb-containing serum resulted in a significant reduction in urine volume per void as compared to the WT serum-treated mice (shown as urine volume per void index, Fig. 4B), but no reduction in body weight, demonstrating that AUAb inhibits the growth of the bladder capacity. The bladder from mice 1 week after last of 4 injections of AUAb-positive sera

A

Upregulated in PCR array of cDNA from the bladder tissue ††	Upregulated in cytokine array of the urine †
Tnf / Tnfα *Il1b* / Il-1β	
Il2ra	GM-Csf
Icos	Il-1a
Socs1	G-Csf
Vcam1	Rantes
	Mip-1b

† p<0.05
†† p<0.01

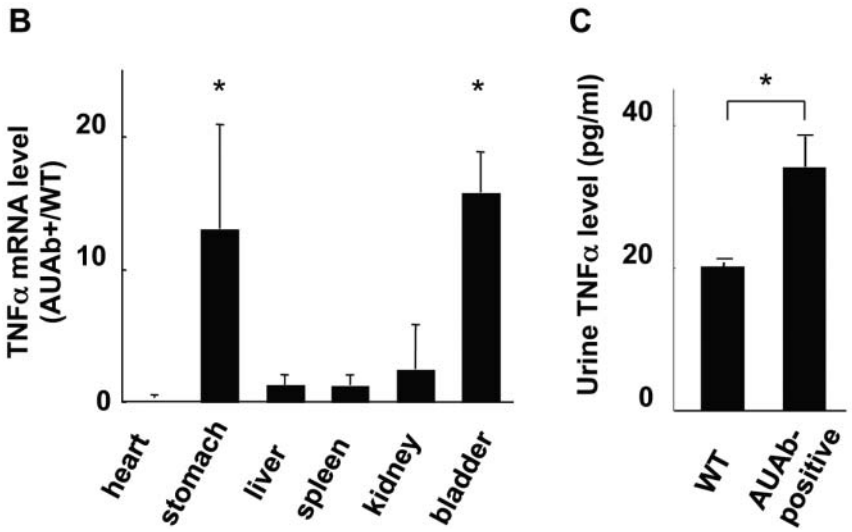

Figure 3 | Higher level of TNFα is detected in the bladder and the urine of AUAb-positive DKO mice. (A) TLDA indicated that mRNA expression level of six inflammatory molecules was significantly upregulated in the bladder of AUAb-positive mice compared to WT mice (†† $p<0.01$). Urine protein assay also revealed that seven inflammatory proteins were significantly upregulated in the urine of AUAb-positive DKO mice compared to WT mice († $p<0.05$). IL-1β and TNFα were expressed higher in both. (B) TNFα mRNA was elevated in the stomach and bladder of AUAb-positive DKO mice (*$p<0.05$). (C) ELISA assay for mouse TNFα has revealed that AUAb-positive DKO mice urine samples contain significantly higher level of TNFα than WT mice (*$p<0.05$).

(Fig. 4C upper right) showed disarrangement of urothelial plaque, which was not observed in mice after injection of control serum (Fig. 4C upper left). The intensity of staining for UPKIIIa was reduced in the urothelial layer of the bladder of mice after injection of AUAb-containing serum (Fig. 4C lower left) compared to the bladder of mice after injection of control serum (Fig. 4C lower right).

Discussion

The present study demonstrates that BALB/c-*Fcgr*2b$^{-/-}$*Pdcd*1$^{-/-}$ mouse (the DKO mouse) expressing AUAb is a novel animal model for autoimmune cystitis. AUAb-positive DKO mouse is a novel disease phenotype exhibiting three distinct features: disarrangement of urothelial layer, inflammation in the suburothelial layer and reduced functional bladder capacity.

The association of AUAb and these three findings could be explained by various possible mechanisms. First intriguing association is found between disarranged urothelial layer and inflammation in the suburothelial layer. Infiltration of the inflammatory cells could be explained either as inflammation directly following antibody-antigen reaction in the urothelial layer, or as consequence after disruption of impermeable barrier function by the urothelium against ions, water and urea[21], which entails infiltration of urine into interstitium of the bladder. The target of AUAb, uroplakin is known as a critical factor for urothelial barrier function[7–9]. *Upk3a* knockout mice have a degenerated leaky urothelium[9], and *Upk2* knockout mice show a frequent urination pattern with reduced urine volume per void[11]. Since AUAb-positive DKO mice show similar phenotypic changes such as degenerated urothelium and reduced urine volume per void in this study (Fig. 1 and Fig. 4A, B and C), alterations in the morphological and functional properties of AUAb-positive DKO mice could be attributable to degenerated, leaky bladder urothelium associated with AUAb.

The other interesting phenotype is reduction in functional bladder capacity of AUAb-positive DKO mice. Although these mice are genetically modified, the reduction of the capacity does not seem to be congenital, but most likely attributable to appearance

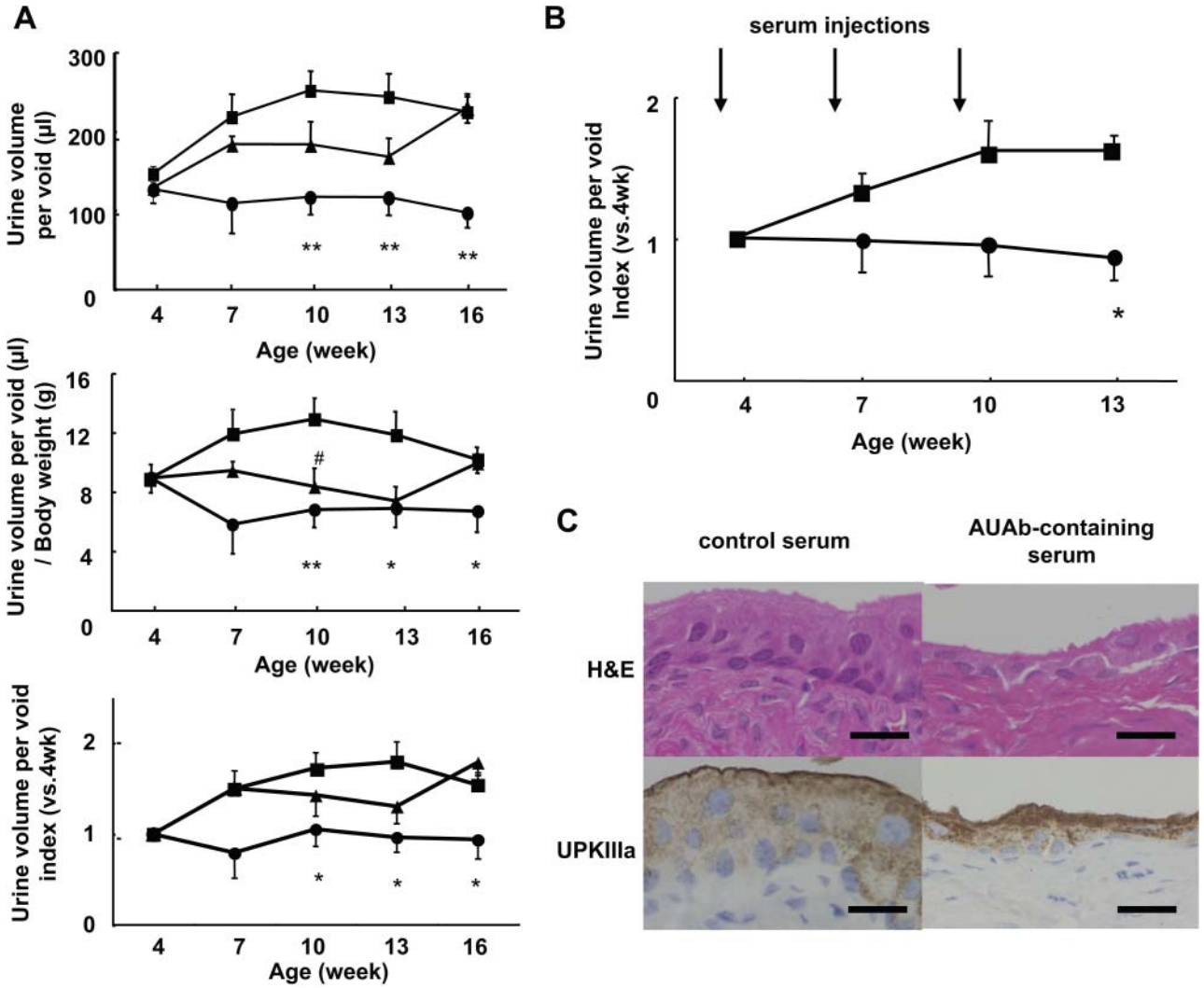

Figure 4 | AUAb-containing serum is pathogenic to bladder storage function. (A) Urine volume per void of female AUAb-positive DKO mice (●: n=7), female AUAb-negative DKO mice (▲: n=6), and female WT mice (■: WT, n=10) was recorded from 4-week-old to 16-week-old by the VSOP method. From 10 to 16-week-old, there were significant differences (**$p<0.01$) in urine volume per void between AUAb-positive DKO mice and WT mice, although there were no significant differences between AUAb-negative DKO mice and WT mice (upper panel). The data adjusted by body weight are shown in the middle panel and the data shown as urine volume per void index (adjusted at 4-week's urine volume per void) are in the lower panel. There were also significant differences between AUAb-positive DKO (●) and WT (■) from 10 to 16-week-old (*$p<0.05$), although there were no significant differences between AUAb-negative DKO (▲) and WT (■) except the urine volume adjusted by body weight at 10-week-old (#$p<0.05$). (B) Serum samples from AUAb-positive DKO mice (●, n=5) and serum samples from WT mice (■, n=5) were injected into WT female mice intraperitoneally (300 μl/body at 4-, 7-, 10-week-old; arrow). The urine volume per void recorded by VSOP method revealed a significant decrease of urine volume per void by administration of the serum from AUAb-positive DKO mice, compared with the serum from WT mice (shown as urine volume per void index). Data are expressed as means ± SE for each group. (C) H&E staining of the mouse bladder after injection of AUAb-containing serum (upper right) showed the disarrangement of urothelial plaque, which was not observed in the bladder after injection of control serum (upper left). The intensity of staining for UPKIIIa was reduced in the urothelial layer of the bladder of AUAb-containing serum injected mice (lower left) compared to the bladder of control serum injected mice (lower right). Bars indicate 100 μm.

of the AUAb in the serum and conspicuous bladder pathology associated with it for three reasons. First, the capacity of the mice is similar until 4 week, after which AUAb appears. Second, there are distinct difference between AUAb-positive and -negative DKO mice. Last, the AUAb-positive serum alone could induce similar functional impairment in WT mice. The possibility of neurogenic bladder dysfunction caused by inflammation in the spinal cord seemed negative based on results of the histological analysis of spinal cord sections (data not shown), and the inflammatory process producing various cytokines including TNFα in the bladder itself seems to impair bladder function. In this process although its functional role is not determined, TNFα level seems to reflect the localized inflammatory process. It is likely that AUAb causes this process by antigen-antibody reaction, although precise following mechanism is unclear. It is rather unlikely that antibody-dependent cellular cytotoxicity could be the cause for the urothelial destruction, since histologically there is no infiltration of inflammatory cells into urothelium in spite of massive inflammation of the bladder, while the activation of complement pathway may be a subject for future study. However, as a limitation of our study, we cannot conclude that AUAb is the only causative factor for the bladder inflammation, as there may be additional factor in sera of AUAb-positive DKO mice causing cystits, and we could not purify the immunoblobulin for sera transfer experiments for technical reason, although important cytokine such as TNFα was undetectable in the serum of AUAb-positive mice.

In behavioral level, the inflammation does not inhibit growth of the bladder itself, since the net wet weight of the retrieved bladders was not different between each group (data not shown). The other more likely possibility is that the inflammation makes animals feel urinary fullness or pain more keenly and frequently, as seen in the clinical patients with bladder inflammation, although there was no sign of bladder pain such as lower abdominal licking or freezing on the AUAb-positive DKO mice.

By any mechanism, the AUAb was shown to play a key role in inducing the bladder dysfunction seen in DKO mice, but translational potential of this model to human pathology is still elusive. There are features in this model resembling pathological processes of human disease like interstitial cystitis or lupus cystitis. For example, AUAb-positive DKO mice had increased number of c-kit positive cells and activated B cells in the bladder. C-kit has been known as a marker for mast cells[16], and degranulation of mast cells results in release of chemical mediators such as histamine or nerve growth factor, reportedly linked to neural changes in humans with interstitial cystitis[20]. However, we could not conclude morphologically that the c-kit positive cells in the AUAb-positive DKO mice are definitely mast cells, and yet little is known about the precise functional role of c-kit-positive cells in bladder diseases. Though there is also a report about activated B cells in the bladder submucosal lesion of interstitial cystitis patients[22], the pathological features of the animal is radically different from clinical interstitial cystitis in human. Beside this, the most different point from the human pathology is the presence of autoantibodies against urothelium, which have not been reported in human patients. At the same time, it is also unlikely that AUAb exists in human at the detrimental level as seen in the DKO, since development of hydronephrosis itself is rarely seen in non-bacterial inflammatory diseases of the urinary tract. We can predict from our findings that, if AUAb exists in the human bladder diseases, it should appear either in a extremely limited number of severest cases, or just transiently at a lower level than seen in DKO mice.

Experimentally, the pathophysiology of AUAb-positive DKO mice presents a novel animal model of bladder pathology: bladder inflammation associated with autoantibody and behavioral phenotype. Our system is distinct from reported autoimmune cystitis models in several aspects[4–6,12]. The reported models failed to show either change in behavioral phenotype[5,6] , histological changes in the urothelium[12], or a characterized pathogenic factor as AUAb[4], all of which are seen in our AUAb-positive DKO mice. Moreover, the appearance of AUAb does not require stimulation of exogenous material such as ovalbumin for sensitization, showing that defective tolerance mechanism itself is enough to induce spontaneous sensitization against urothelium, generating potent autoantibody to alter the micturiton behavior. In summary, the AUAb-positive DKO mouse demonstrates that autoimmunity can induce significant impairment of the bladder function.

In conclusion, this report characterizes a novel comprehensive mouse model of autoantibody-associated cystitis, which provides various insights about establishment of the bladder autoimmunity.

Methods

Animals. Wild-type BALB/c mice were purchased from Clea Japan, Inc. (Tokyo, Japan). BALB/c- *Pdcd*1$^{-/-}$ and BALB/c- *Fcgr*2b$^{-/-}$ mice were kindly provided by Drs. Tasuku Honjo (Kyoto University), Jeffrey V. Ravetch (Rockefeller University), and Toshiyuki Takai (Tohoku University)[13,23]. BALB/c- *Fcgr*2b$^{-/-}$ *Pdcd*1$^{-/-}$ mice were produced as we described previously[14]. The Institute of Laboratory Animals at the Kyoto University Graduate School of Medicine approved all mouse protocols. All animals were maintained under specific pathogen-free conditions.

Immunofluorescence (IF). The existence of AUAb in the serum of mice was examined by utilizing it as a primary antibody of IF for mouse bladder section. The bladder tissues were collected from wild-type BALB/c mice, which were snap frozen in the OCT compound. Cryosections were fixed with CytoFix (BD Biosciences, CA, USA) and incubated with x100 diluted serum from mice, followed by FITC labeled anti–mouse IgG Ab (Jackson ImmunoResearch Laboratories, Inc., PA, USA). Sections were examined with an Eclipse E1000M microscope (Nikon, Tokyo, Japan).

Immunoblotting. Mouse UPKIIIa partial cDNA (corresponding to W19 to A125) was subcloned into pGEX-6P-1 vector (GE Healthecare, Buckinghamshire, UK) and GST-fusion protein of mouse UPKIIIa (GST-UPKIIIa) was expressed and purified according to the manufacturer's instruction[14]. The purified solution (20 μg) was boiled for 5 min in a SDS sample buffer solution and separated by SDS-PAGE on a 10% Tris-HCl mini gel and transferred onto a polyvinylidene difluoride membrane following standard methods. Membranes were incubated with x100 diluted mouse serum or mouse monoclonal antibody (mAb) against UPKIIIa (PROGEN, Heidelberg, Germany) for two hours at room temperature and visualized by F(ab2)' fragment of goat anti-mouse IgG (Jackson Immuno Research, PA, USA) with enhanced chemiluminescent detection system (GE Healthcare, Buckinghamshire, UK).

Immunohistochemistry (IHC) and scanning electron microscopy. Bladder tissues were collected after emptying the bladder of mice by pressing their lower abdomen. The following antibodies were used: anti-UPKIIIa (PROGEN, Heidelberg, Germany), anti-c-kit (Novocastra, Newcastle, UK), anti-TNFα (Santa Cruz, CA, USA), anti-CD11c and anti-F4/80 (Abcam, MA, USA), anti-CD4 (BD Pharmingen, CA, USA), anti-B220 (eBioscience, CA, USA). Tyramide signal amplification-avidin-biotin complex (TSA-ABC) method was used for IHC[24]. Sections were examined with an Eclipse E1000M microscope (Nikon, Tokyo, Japan). For scanning electron microscopy, bladders were fixed with 2% glutaraldehyde in 0.1 M phosphate buffer (pH 7.2), postfixed with 1% OsO_4 and 0.1 M sucrose in 0.1 M phosphate buffer[25] and examined by using an electron microscope (Hitachi H7000, Tokyo, Japan).

RNA isolation and quantitative RT-PCR. RNA was isolated from mouse organs using the RNeasy mini kit (Qiagen, CA, USA). Whole bladders were used. RNA (1 μg) was reverse-transcribed using the First-Strand cDNA synthesis kit (Amersham Pharmacia Biotech, NJ, USA), following manufacturer's protocol. Quantitative real-time PCR with SYBR Green PCR Master Mix (Applied Biosystems, CA, USA) was done using the GeneAmp 5700 Sequence Detection System (Applied Biosystems, CA, USA) with the relative standard curve method, at 95°C for 15 seconds and 60°C for 1 minute. PCR efficiency was examined by serially diluting the template cDNA and the melting curve data were collected to check the PCR specificity[26]. No PCR product was detected in control samples in which reverse transcriptase was omitted. An internal loading control of glyceraldehyde-3-phosphate dehydrogenase (GAPDH) expression was used for all genes of interest. Results were quantified using the relative standard curve method. The primers used were as follows: GAPDH (452 bp) sense, 5′-ACCACAGTCCATGCCATCAC-3′, and antisense, 5′-TCCACCACCCTGTTGCTGTA-3′; TNFα (60 bp) sense, 5′-CCCTCACACTCAGATCATCTTCT -3′, and antisense 5′-GCTACGACGTGGGCTACAG -3′. Each PCR regimen involved 5 minutes of initial denaturation step at 95°C followed by 38 cycles at 94°C for 60 seconds, 60°C (TNFα) or 65°C (GAPDH) for 60 seconds, and 72°C for 1 minute and 30 seconds.

TaqMan low-density array (TLDA). Gene expression analysis was performed using TaqMan immune-profiling/inflammation low-density arrays (Applied Biosystems, CA, USA), according to manufacturer's protocol. Real time RT-PCR amplification was performed on an ABI Prism 7900 H.T. Sequence Detection system (Applied Biosystems, CA, USA). Thermal cycling conditions were as follows: 2 minutes at 50°C, 10 minutes at 94.5°C, and for 40 cycles, 30 seconds at 97°C and 1 minute at 59.7°C. TLDA cards were analyzed with relative quantification (RQ) documents and RQ manager software for automated data analysis (Applied Biosystems, CA, USA). Glyceraldehyde-3-phosphate dehydrogenase (GAPDH) was selected as the internal control.

Urine cytokine assay. Inflammatory cytokine concentrations in urine samples from AUAb-positive DKO and WT mice were analyzed by Bio-Plex Mouse Cytokine Group I 23-Plex (Bio-Rad, PA, USA) according to the manufacturer's instruction.

TNFα ELISA assay. TNFα concentration in mice urine samples were analyzed by another ELISA assay, Mouse TNFα ELISA (eBioscience, CA, USA), according to the manufacturer's instruction.

Voided Stain on Paper (VSOP) method. Voiding behavior of mice was analyzed as described previously[15]. Briefly, the mice were fed with 50 μl/g of distilled water via gastric tube and placed on a screen above the filter paper, and their urination was recorded over two hours. The recorded stain areas were copied to another paper and calculated to the volume by computer software Photoshop (Adobe, USA). Age-dependent changes in bladder volume were also evaluated, either as net volume, volume adjusted to body weight, or using the urine volume per void index calculated as the ratio of urine volume per void of 4, 7, 10, 13 or 16-week-old mice against that of 4-week-old mice.

Pathogenicity test of the AUAb-containing serum. Test serum samples were pooled from 20 DKO mice at 16 to 20-week-old, and confirmed to have AUAb by IF. Control serum samples were pooled from 15 age-matched BALB/c wild-type mice. These serum samples were preserved at −80°C. The pooled serum (300 μl/body) was then injected intraperitoneally to WT female mice at 4, 7 and 10-week-old (n=5 for each group). Urine volume per void was assesse by VSOP method at 4, 7, 10, and 13-week-old. On the other session, the serum was injected on the WT mice at 4, 7, 10, and

13-week-old and the bladder tissues were collected one week after the last injection and evaluated histologically.

Statistical analysis. Results are expressed as means ± SE. Statistical comparisons between two experimental groups were performed by Student's paired and unpaired *t*-test using Statview 5.0 (SAS institute, Inc., NC, USA), and P value <0.05 was considered as significant.

1. van de Merwe, J. P. Interstitial cystitis and systemic autoimmune diseases. *Nat Clin Pract Urol.* **4**, 484–491 (2007).
2. Alarcón-Segovia, D., Abud-Mendoza, C., Reyes-Gutiérrez, E., Iglesias-Gamarra, A. & Díaz-Jouanen, E. Involvement of the urinary bladder in systemic lupus erythematosus. A pathologic study. *J Rheumatol.* **11**, 208–210 (1984).
3. Popescu, O. E., Landas, S. K. & Haas, G. P. The spectrum of eosinophilic cystitis in males: case series and literature review. *Arch Pathol Lab Med.* **133**, 289–294 (2009).
4. Saban, R. *et al*. Differential release of prostaglandins and leukotrienes by sensitized guinea pig urinary bladder layers upon antigen challenge. *J Urol.* **152** (**2 Pt1**), 544–549 (1994).
5. Liu, W., Deyoung, B. R., Chen, X., Evanoff, D. P. & Luo, Y. RDP58 inhibits T cell-mediated bladder inflammation in an autoimmune cystitis model. *J Autoimmun.* **30**, 257–265 (2008).
6. Liu, W., Evanoff, D. P., Chen, X. & Luo, Y. Urinary bladder epithelium antigen induces CD8+ T cell tolerance, activation, and autoimmune response. *J Immunol.* **178**, 539–546 (2007).
7. Lavelle, J. *et al*. Bladder permeability barrier: recovery from selective injury of surface epithelial cells. *Am J Physiol Renal Physiol.* **283**, F242–253 (2002).
8. Kong, X. T. *et al*. Roles of uroplakins in plaque formation, umbrella cell enlargement, and urinary tract diseases. *J Cell Biol.* **167**, 1195–1204 (2004).
9. Hu, P. *et al*. Role of membrane proteins in permeability barrier function: uroplakin ablation elevates urothelial permeability. *Am J Physiol Renal Physiol.* **283**, F1200–1207 (2002).
10. Hu, P. *et al*. Ablation of uroplakin III gene results in small urothelial plaques, urothelial leakage, and vesicoureteral reflux. *J Cell Biol.* **151**, 961–972 (2000).
11. Hodges, S. J. *et al*. Voiding pattern analysis as a surrogate for cystometric evaluation in uroplakin II knockout mice. *J Urol.* **179**, 2046–2051 (2008).
12. Altuntas, C. Z. *et al*. Autoimmunity to Uroplakin II Causes Cystitis in Mice: A Novel Model of Interstitial Cystitis. *Eur Urol.* Jun 28 (2011).
13. Nishimura, H. *et al*. Autoimmune dilated cardiomyopathy in PD-1 receptor-deficient mice. *Science.* **291**, 319–322 (2001).
14. Okazaki, T. *et al*. Hydronephrosis associated with antiurothelial and antinuclear autoantibodies in BALB/c-Fcgr2b-/-Pdcd1-/- mice. *J Exp Med.* **202**, 1643–1648 (2005).
15. Sugino, Y. *et al*. Voided stain on paper method for analysis of mouse urination. *Neurourol Urodyn.* **27**, 548–552 (2008).
16. Pang, X., Sant, G. & Theoharides, T. C. Altered expression of bladder mast cell growth factor receptor (c-kit) in interstitial cystitis. *Urology.* **51**, 939–944 (1998).
17. Kollias, G., Douni, E., Kassiotis, G. & Kontoyiannis, D. The function of tumour necrosis factor and receptors in models of multi-organ inflammation, rheumatoid arthritis, multiple sclerosis and inflammatory bowel disease. *Ann Rheum Dis.* **58** Suppl 1, I32–I39 (1999).
18. Rutgeerts, P., Vermeire, S. & Van Assche, G. Biological therapies for inflammatory bowel diseases. *Gastroenterology.* **136**, 1182–1197 (2009).
19. Batler, R. A., Sengupta, S., Forrestal, S. G., Schaeffer, A. J. & Klumpp, D. J. Mast cell activation triggers a urothelial inflammatory response mediated by tumor necrosis factor-alpha. *J Urol.* **168**, 819–825 (2002).
20. Chen, M. C., Keshavan, P., Gregory, G. D. & Klumpp, D. J. RANTES mediates TNF-dependent lamina propria mast cell accumulation and barrier dysfunction in neurogenic cystitis. *Am J Physiol Renal Physiol.* **292**, F1372–F1379 (2007).
21. Chang, A., Hammond, T. G., Sun, T. T. & Zeidel, M. L. Permeability properties of the mammalian bladder apical membrane. *Am J Physiol.* **267**, C1483–C1492 (1994).
22. Harrington, D. S., Fall, M. & Johansson, S. L. Interstitial cystitis: bladder mucosa lymphocyte immunophenotyping and peripheral blood flow cytometry analysis. *J Urol.* **144**(4), 868–71 (1990).
23. Bolland, S. & Ravetch, J. V. Spontaneous autoimmune disease in Fc(gamma)RIIB-deficient mice results from strain-specific epistasis. *Immunity.* **13**, 277–285 (2000).
24. Toda, Y. *et al*. Application of tyramide signal amplification system to immunohistochemistry: a potent method to localize antigens that are not detectable by ordinary method. *Pathol Int.* **49**, 479–483 (1999).
25. Luft, J. H. Improvements in epoxy resin embedding methods. *J Biophys Biochem Cytol.* **9**, 409–414 (1961).
26. Matsui, Y. *et al*. Sensitizing effect of galectin-7 in urothelial cancer to cisplatin through the accumulation of intracellular reactive oxygen species. *Cancer Res.* **67**, 1212–1220 (2007).

Acknowledgement

This work was supported by Grant-in-aid for Scientific Research from JSPS 20659249 and 20390425, Young Investigators Award from Japanese Urological Association (to YS), a grant from Japanese Ministry of Health, Labor and Welfare (to SK), and Shimizu Foundation for Promotion of Immunology grant (to AK).
The authors thank Drs Takeshi Soda, Toshinari Yamazaki, Yoshinobu Toda, and Mikio Furuse for their valuable technical support and advice.

Author contributions

Drs. Sugino Y, Nishikawa N and Kanematsu A have planned and performed the study, and prepared majority of the manuscript. Drs. Yoshimura K, Kuno S, Yoshimura N and Okazaki T gave us contributions to conception and design of the study. Dr. Ogawa O gave us a general guidance and support of the study as laboratory director. All authors reviewed the manuscript.

Additional information

Supplementary information accompanies this paper at http://www.nature.com/scientificreports

Competing financial interests: The authors declare no competing financial interests.

How to cite this article: Sugino, Y. *et al*. BALB/c-*Fcgr2b*$^{-/-}$*Pdcd1*$^{-/-}$ mouse expressing anti-urothelial antibody is a novel model of autoimmune cystitis. *Sci. Rep.* **2**, 317; DOI:10.1038/srep00317 (2012).